Journal of Nuclear Materials 390–391 (2009) 671–676

Contents lists available at ScienceDirect

Journal of Nuclear Materials

journal homepage: www.elsevier.com/locate/jnucmat

Surface temperature effects on the retention and pressure variation in continuous and cyclic plasma exposures on the tungsten

K. Okamoto [a], H. Zushi [b,*], Y. Hirooka [c], R. Bhattacharyay [a], M. Sakamoto [b], M. Sato [c]

[a] Interdisciplinary Graduate School of Engineering Science, Kyushu University, Kasuga 6-1, Fukuoka 816-8580, Japan
[b] RIAM, Kyushu University, 87, Kasuga, Fukuoka 816-8580, Japan
[c] NIFS Oroshi, Toki, Gifu 509-5292, Japan

ARTICLE INFO

PACS:
52.40.Hf
39.30.+w
68.43.Vx

ABSTRACT

Hydrogen retention and pressure variation in and from the inert gas plasma sprayed tungsten (IPS-W) exposed to plasmas are described. Two kinds of plasma irradiation scenarios are investigated in continuous and cyclic exposures. The H retained fluence at the surface temperature T_s of 470–900 K was evaluated in the range of 4×10^{20}–2×10^{22} H/m^2 for the bombarding fluence of 1×10^{24}–1×10^{26} H/m^2 under continuous exposure condition. For the cyclic exposure, it is found that if $\Delta T_s > 100$ K during exposure, the apparent re-emission (pressure increase) is triggered by both ΔT_s and irradiation itself, and just after the exposure it turns to apparent retention (pressure decrease). However, for $\Delta T_s < 40$ K no apparent re-emission and retention are observed in the cycle. This fact suggests that the hydrogen reemission is enhanced during the exposure via the surface recombination process depending on ΔT_s or T_s gradient across the specimen.

1. Introduction

Plasma facing material (PFM) used for International Thermonuclear Experimental Reactor (ITER) has been reviewed from a fusion reactor PFM point of view [1]. Tungsten is a candidate material since it has a high threshold for sputtering as well as a very high melting temperature. Furthermore, for particle recycling, it has been also known that the release of H_2 from the tungsten surface is dominated by its endothermic properties in TEXTOR [2]. For the surface temperature T_s dependence of the hydrogen retention in tungsten, there are several reports [3–6]. The tritium retention has a maximum at intermediate temperatures, interpreted by enhanced diffusion in the implanted range, in 100 eV triton implantation experiments [3], and relatively lower temperature (~600 K) needed for release of deuterium is ascribed to smaller trapping energy (~1.5 eV) compared with graphite [4]. The fluence dependence (up to 10^{25} D$^+$/m^2) shows that retention at 500 K is larger than that at 300 K and no saturation is observed at 500 K. The deuteron profile measurements in tungsten [7–9] show that they diffuse deep into tungsten whose range exceeds the implantation range by two orders of magnitude and suggest an enhanced diffusion mechanism. The blister is formed as T_s increases and the size reaches ~30 μm. However, no blister formation is observed at T_s above 680 K [9]. It has been suggested in Ref. [7] that hydrogen will accumulate in tungsten if the recovery time between two shots is shorter than the time needed for the release of solute hydrogen. Actually, for long pulse operation of the tokamak plasma it has been found that the difficulty of the particle control is due to the temporal change in re-emission and retention properties from and in the plasma facing components PFCs, on which the heat load are deposited non-uniformly [10–12]. It has been also reviewed that in long pulses the particle recovery after shot is independent of the retained fuel, leading to a significant wall inventory build up in contrast with short pulses [13,14].

Thus, understanding of the re-emission and retention processes of H_2 from and in tungsten as a function of ion fluence and surface temperature is essential for not only the tritium inventory, but also for the density control in steady state reactors. In order to control the shot history or shot accumulation effects, dynamic aspects of re-emission and retention from and in the PFCs should be clarified. Two kinds of exposure modes, namely 'continuous exposure' and 'cyclic exposure with a recovery time', are examined for IPS-W whose surface temperature is within the range of 470–900 K. The purposes of this work are to study hydrogen retention in the former mode at the particle flux 1×10^{21}–8×10^{21} H/m^2/s and in the latter mode to investigate the pressure variation as a function of T_s in ECR plasma.

2. Experimental procedure

A linearly magnetized steady state plasma facility VEHICLE-1 [15] is used for plasma exposure experiment, as shown in Fig. 1. Using the 2.45 GHz power source steady state hydrogen and he-

* Corresponding author.
E-mail address: zushi@triam.kyushu-u.ac.jp (H. Zushi).

0022-3115/$ - see front matter © 2009 Elsevier B.V. All rights reserved.
doi:10.1016/j.jnucmat.2009.01.312

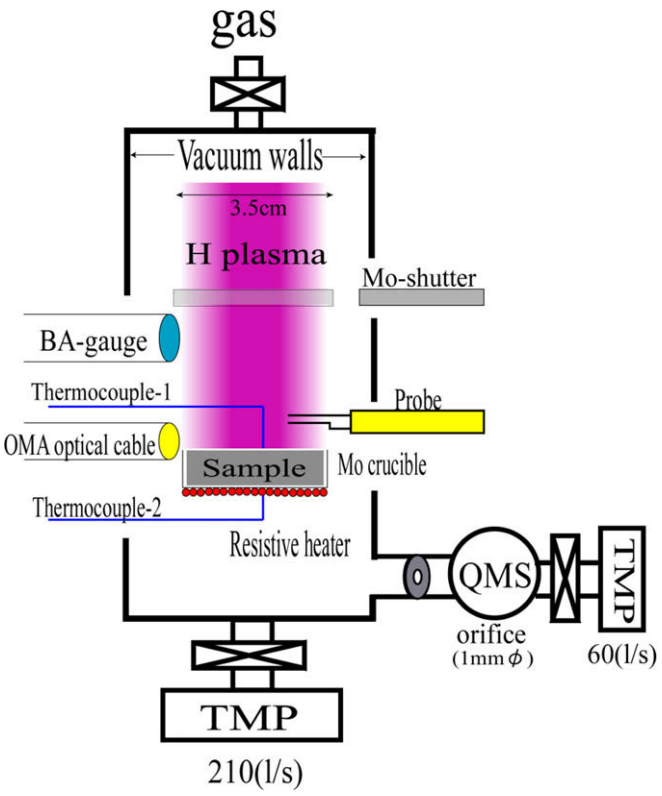

Fig. 1. Schematic view of VEHICLE-1.

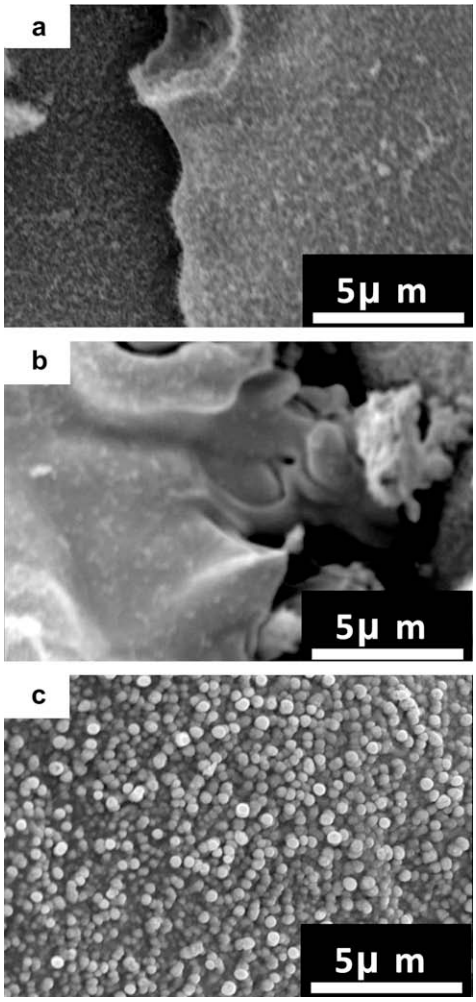

Fig. 2. SEM micrographs showing surface morphology of IPS-W; (a) before exposure, (b) after H exposure, and (c) the combined exposure for H and He plasmas.

lium plasmas are generated at second harmonic electron cyclotron resonance heating. The actual diameter of the plasma column is about 35 mm limited by a donut plate made of tantalum, positioned upstream of a specimen, which is a tungsten coated stainless steel disk of 3 mm in thickness and 28 mm in diameter. Tungsten with a thickness of ~0.5 mm is coated by inert gas plasma spray method on this disk. The IPS coating is produced by plasma spraying in argon atmosphere at atmospheric pressure and surface roughness is ~50 μm. The IPS-W specimen is set in a sample tray made of molybdenum and the rear side of this tray is heated by heat conduction from a resistive heater. The temperatures at both front (surface) and rear sides are recorded with thermocouples at the time resolution of 1–5 s. Thus, T_s is controlled or varied during plasma exposure. In order to control the exposure scenario both the shutter on/off and rf on/off techniques are adopted. The pneumatic Mo shutter is used to keep the plasma and environment conditions constant and for latter case, the gas condition is fixed. The bombarding energy is controlled by biasing the sample tray with DC bias voltages (0–250 V). The implantation range of protons is ~ a few nm. At zero bias voltage, bombarding energy is less than 25 eV. A scanning Langmuir probe is used for plasma density (3.3×10^{15}–2.6×10^{16} m^{-3}) and electron temperature (3.6 eV–7.3 eV) measurements. These parameters are controlled by rf power. The density and electron temperature profiles are rather flat over the area within the limited diameter. From the operation characteristics the following fraction ratio $H:H_2:H_3 = 0.1:0.3:0.6$ is used to evaluate the ion bombarding flux Γ_{ion}, ranging from 1.3×10^{21} to 7.8×10^{21} H-ions/m^2/s. Typically, the neutral pressure in the main chamber is ~0.13 Pa during plasma operation. The base pressure is $<1.3 \times 10^{-6}$ Pa. A quadruple mass spectrometer (QMS) is housed in a differentially pumped vacuum chamber separated from the main chamber by an orifice creating a pressure ratio of about 250:1 at 0.13 Pa of the main chamber. Although thermal transpiration effects has to be considered to evaluate the pressure ratio when gas temperatures in two chambers are different, it can be assumed that continuous fuelling H_2 gas at room temperature keeps the gas temperature difference low. Thus, the calibration is done by means of D_2 standard leak (1.3×10^{13} D_2/s) attached in the main chamber. The H_2 partial pressure P_{H_2} and others ($P_{H_2O}, P_{CH_4}, P_{CO_2}$ etc.) are recorded at every ~2.5 s. During the plasma exposure P_{H_2} is $\sim 4 \times 10^{-3}$ Pa, $P_{H_2O} \sim 4 \times 10^{-6}$Pa and $P_{CH_4} \sim P_{CO_2} \sim 4 \times 10^{-7}$Pa. It has been pointed out in Ref. [7] that the inventory measured by thermal desorption spectrometry TDS depends very critically on the time between the exposure termination and the onset of TDS due to the decrease of the solute inventory after the termination of exposure. Without a time delay after plasma exposure or air vent post-exposure TDS and isothermal desorption measurements have, therefore, been performed by using the heater in the same facility. The maximum temperature is 1150 K. The contribution of out gassing from the environment is carefully subtracted. Determination of the zero flux level (re-emission flux = retention flux) in cyclic plasma exposure experiment is relatively difficult compared with that of ion beam bombardment experiment [8], in which background of masses (D and DH) before starting and after finishing the D beam implantation has been subtracted. In the present study the zero level of ΔP_{H_2} during the cyclic exposure scenario has been obtained during the exposure off cycle using fast Fourier transform FFT and event averaging technique. We recognize from our results

that the present calibration technique is inadequate under the high temperature conditions. In Ref. [16] the ro-vibrational temperature measurement have been performed to evaluate the temperature of H_2 released from a hot spot on the limiter. Although this kind of spectroscopic measurement of H_2 is useful, the effects of neutral temperature in the high specimen temperature experiment are beyond the scope of the present study.

3. Experimental results and discussion

Surface morphologies of IPS-W specimen, obtained from the scanning electron microscopy, SEM, are shown in Fig. 2. These were taken before experiments (a) and after H plasma exposure (b). No essential difference is observed between two. In particular, result for a combined exposure to hydrogen and helium plasmas is

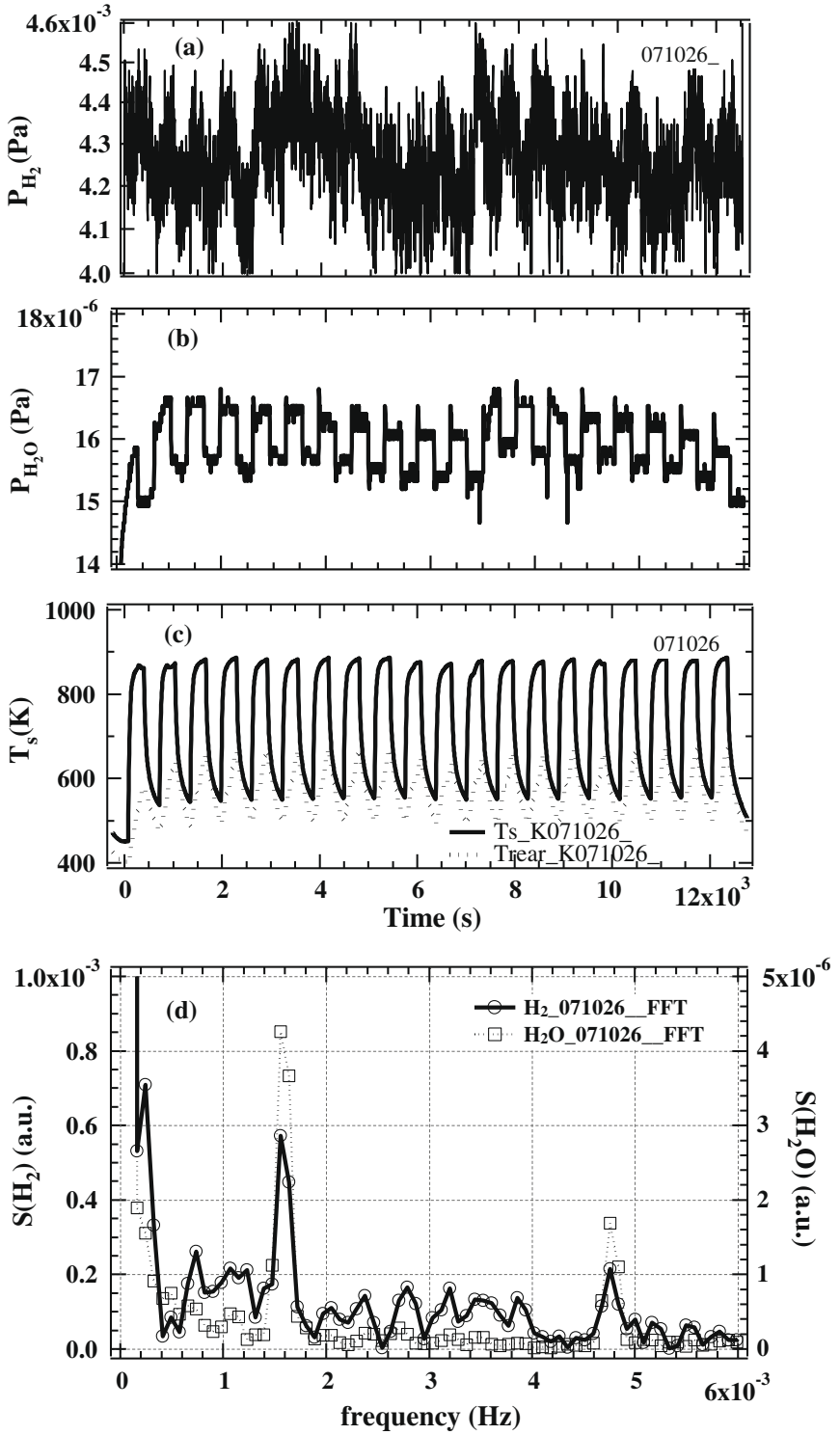

Fig. 3. Particle release and T_s in 'cyclic exposure with a recovery time' mode; (a) P_{H_2}, (b) P_{H_2O}, (c) T_s (solid) and T_{rear} (dotted), (d) FFT spectra of P_{H_2} (t) (circles and solid) and P_{H_2O} (t) (squares and dotted). Cyclic exposure sequence is τ_{on}/τ_{off} = 5 min/5 min.

shown in (c). The experimental sequence is as follows: (1) annealing at T_s = 827 K for 30 min, (2) H plasma exposure at the bias voltage of 250 V and rf power of 500 W, (3) TDS up to 827 K after stopping exposure, and then (4) He plasma exposure at zero bias voltage and 800 W for about one hour. These experiments are repeated sequentially under different continuous H-plasma exposure conditions. Total fluence of H is 3×10^{25} H/m^2 at the flux 5×10^{20} H/m^2/s for total integrated exposure time of 12 h and fluence of He is 2×10^{24} He/m^2 at the flux 7×10^{19} He/m^2/s for total 7.5 h. Many bubbles whose size is <1 μm are found. The details will be reported elsewhere. Similar results have been reported for pre-implantation of He$^+$ experiments at the energy of 8 keV at low fluence of 2×10^{21} He/m^2 [17].

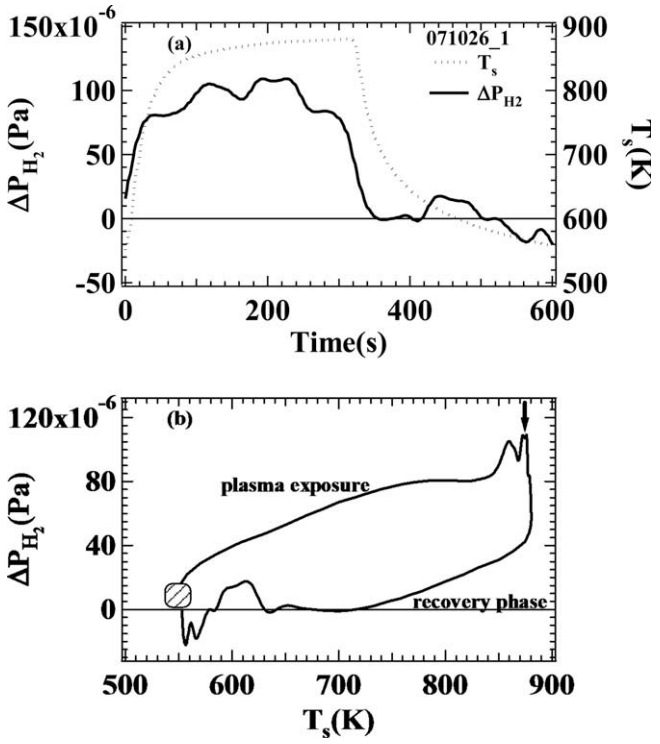

Fig. 4. (a) Using an event averaging technique, $<P_{H_2}>$ and $<T_s>$ are averaged during each cycle, and (b) a hysteresis relation between $<P_{H_2}>$ and $<T_s>$. A shaded point indicates the start of exposure and an arrow the end of the exposure.

Fig. 3 shows example of the pressure and T_s variation in 'cyclic exposure with a recovery time' mode. In this case, both exposure and recovery times are 300 s (τ_{on}/τ_{off} = 300s/300s) and twenty cycles are repeated by using the shutter. During the recovery phase, the shutter prevents ISP-W specimen from plasma exposure. Although the plasma condition is fixed, T_s is varied from 530 K to 870 K during this cycle, as is similar to actual tokamak operation. As a consequence of the plasma exposure-recovery cycle and ΔT_s = 340 K, P_{H_2} is varied by ~0.7–3.9%. Although the change in P_{H_2O} shows a periodical response and variation is 3.7–6.4%, its contribution to P_{H_2} can be neglect. The FFT technique is applied to analyze the response of the H_2 release, as shown in Fig. 3(d). At f = 1.67 mHz peaks are found on both P_{H_2} and P_{H_2O} signals. These signals are only analyzed.

A relation between averaged H_2 release and averaged T_s variation is studied by an event averaging technique for each exposure cycle. The results are shown in Fig. 4. Here ΔP_{H_2} for each cycle during the exposure phase is obtained by subtracting averaged P_{H_2} during the recovery phase. Thus the temporal variation of P_{H_2} during the whole cycle is neglected. The change in $<\Delta P_{H_2}>$ during the plasma exposure phase is significant and similar to P_{H2O}. The T_s dependence of $<\Delta P_{H_2}>$ shows a clear temperature hysteresis curve characterized by a rapid drop at the maximum T_s. This suggests that the re-emission process is not dominated by T_s only, but both elevation in T_s and plasma irradiation itself.

Fig. 5 shows a relation between apparent reemission (positive) or retention (negative) rate $<\Delta\Phi_{H_2}>$ (H/s) from and in the ISP-W and $<T_s>$ for various exposure duration from 10 to 300 s. Since plasma heats the specimen, T_s is varied from 470 to 900 K in the cycle without feedback control of the heater. When $<\Delta T_s> \geqslant 100$ K, a clear rise in $<\Delta\Phi_{H_2}>$, indicating apparent re-emission, during the exposure phase and reduction along a different curve during the recovery phase are found in a wide range of $<T_s>$ and the exposure duration. Since each symbol is plotted at every 20 s, it is found that the rise time in $<\Delta\Phi_{H_2}>$ is within ~20 s, just after the plasma exposure. During this time $<T_s>$ increases rapidly by at least 100 K. However, for the case of $<\Delta T_s>$ (<40 K), although $<T_s>$ is at the middle range around 640 K no variation in $<\Delta\Phi_{H_2}>$ is observed within $\pm 4 \times 10^{15}$ H/m^2. Furthermore, rectangular response in $<\Delta P_{H_2O}>$, $<\Delta P_{CO_2}>$ and $<\Delta P_{CH_4}>$ is similar to those in $<\Delta T_s>$ (>100 K).This

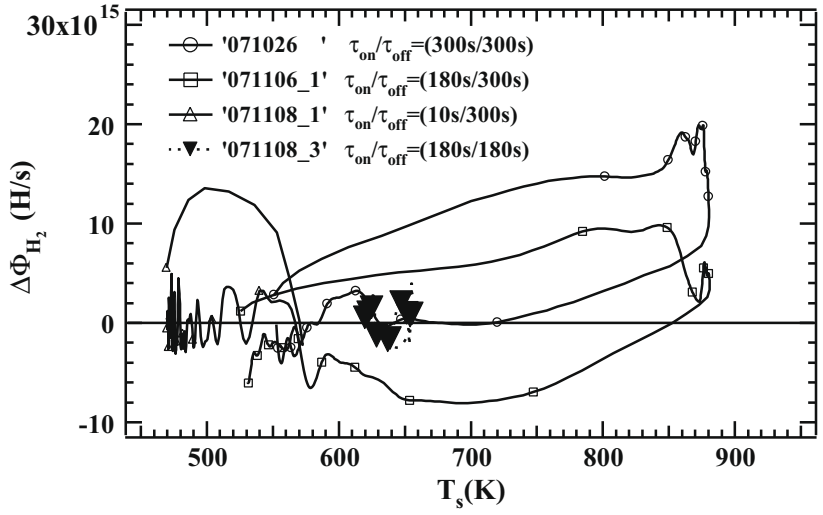

Fig. 5. A relation of $<\Delta\Phi_{H_2}>$ with respect to $<T_s>$ for various combination of on and off times. For case denoted by reverse triangles $<\Delta T_s>$ is controlled by <40 K.

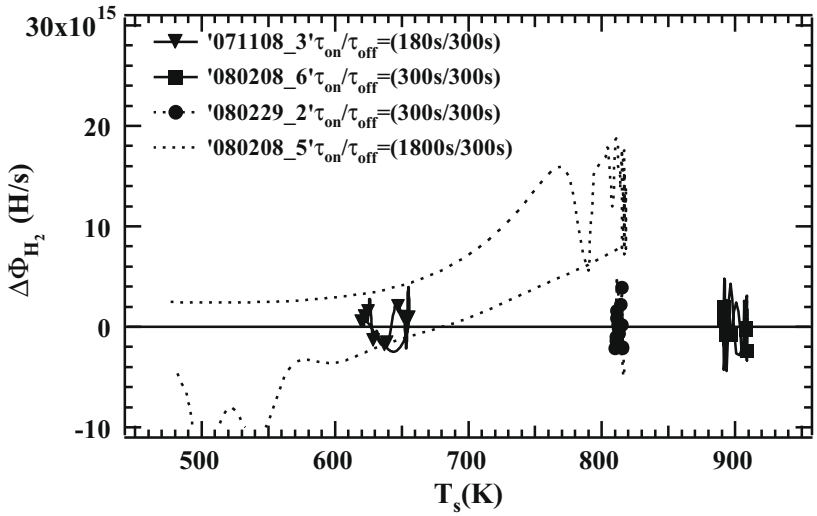

Fig. 6. <$\Delta\Phi_{H_2}$> vs. <T_s> for controlled temperature exposure at various T_s range. For comparison, uncontrolled T_s case for 1800s exposure is also shown by dotted lines.

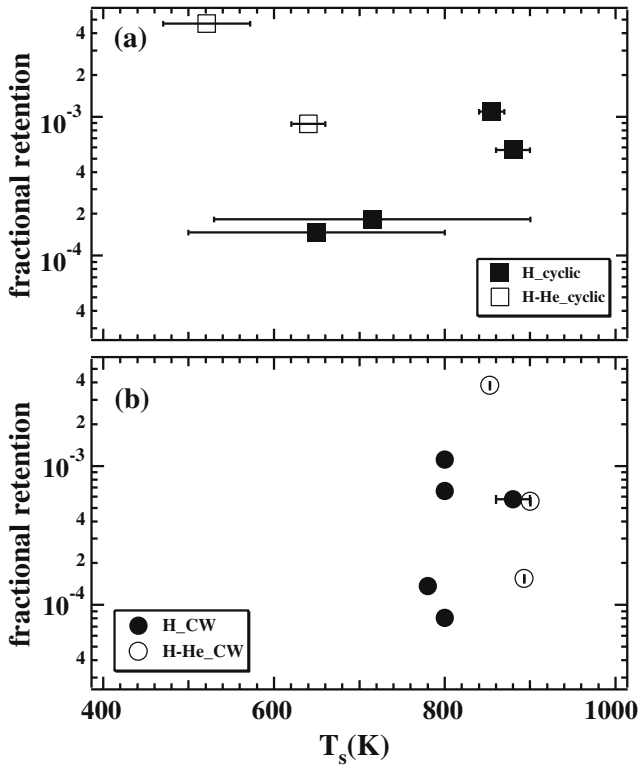

Fig. 7. The fractional retention of hydrogen obtained in continuous and cyclic exposures is plotted as a function of T_s. The combined exposure data for H and He are also shown.

fact suggests that onset of apparent reemission is triggered by both the rise in <ΔT_s> and plasma exposure.

For the case of controlled T_s operation over the cycle, the variation in <$\Delta\Phi_{H_2}$> is studied for various T_s range. The results are shown in Fig. 6. For comparison, data with uncontrolled T_s with τ_{on}/τ_{off} = 1800s/300s are also given. Data during 2–5 cycles are averaged. The heater is controlled to keep T_s constant (<40 K) during the recovery phase. All these data are taken at zero bias voltage in order to keep T_s constant during the plasma exposure phase. The T_{rear} is 950–1150 K and the temperature gradient ∇T_5 across the IPS-W specimen is opposite to that shown in Fig. 5. The order of ∇T_5 is ~100 K/mm. The expected bombarding energy is a sheath acceleration voltage of $3T_e$~15–23 eV. Since no cooling system is installed, only controlled T_s experiments are performed at higher T_s range. The effects of bombarding energy (or very short implantation range), T_s variation and the direction of ∇T_5 are not discriminated in these dataset. These are left for future work.

In Fig. 7 the exposure temperature dependence of the fractional retention of H is compared at fluence from 10^{24} to 10^{26} H/m^2 and over 470–900 K for two exposure scenarios. Horizontal bar indicates the T_s variation during the exposure. Results of cyclic and continuous exposures show the similar retention. Continuously exposed data is higher by factors of 4–10 than data for vacuum plasma sprayed tungsten VPS-W obtained in D_2 plasma exposure [18]. In that experiment, TDS was done after the specimen was removed from the irradiation chamber to TDS facility. When the TDS temperature range was lower than T_s during exposure, the amount of released H was low, as reported in [19]. Therefore, after initial TDS, He irradiation was done and the release of retained H was enhanced during He exposure. The released H from the environment due to He plasma production was subtracted using Mo shutter data. Since the bombarding energy of He is <25 eV, the retained H is expected to be trapped near the top surface. Observed H retention is three to six times larger than that without using helium exposure at the same H fluence. This enhanced retention may relate to the small bubbles (see Fig. 2(c)).

4. Summary

In order to simulate the pulsed tokamak operation and to understand the dynamic response in re-emission and retention during the whole cycle the 'cyclic plasma exposure with the recovery time' mode is used. The partial pressure measurement using differential pumped QMS is performed to follow the pressure change responding to the cyclic exposure. It is found that apparent re-emission is triggered at least within 20 s by both T_s rise and plasma exposure. Immediately after the exposure is switched off, apparent reemission turns to apparent retention during the T_s decay phase. In contrast to the above result, no reemission and dynamic retention are observed in the wide range of T_s under the condition ΔT_s < 40 K, zero bias voltage and negative ∇T_5. The difference in hydrogen retention for two continuous and cyclic modes is not clear, though a drastic difference between single long pulse and shorts pulses is seen in the real tokamak operation. The He plasma exposure is used to evaluate H retention after H plasma

exposure. Observed retention is three to six times larger than that without using helium exposure at the same fluence.

Acknowledgements

This work is performed with the support and under the auspices of the NIFS Collaboration Research Program (NIFS05KUTR009). We would like to acknowledge Professor Tanabe and Professor Yoshida for valuable comments on this work.

References

[1] R.A. Causey, J. Nucl. Mater. 300 (2002) 91.
[2] T. Hirai et al., J. Nucl. Mater. 307–311 (2002) 79.
[3] R.A. Causey et al., J. Nucl. Mater. 266–269 (1999) 467.
[4] C. Garcia-Rosales et al., J. Nucl. Mater. 233–237 (1996) 803.
[5] A.A. Hass et al., J. Nucl. Mater. 258–263 (1997) 889.
[6] A.A. Hass et al., J. Nucl. Mater. 241–243 (1997) 1076.
[7] P. Franzen et al., J. Nucl. Mater. 241–243 (1997) 1082.
[8] V.Kh. Alimov, B.M.U. Scherzer, J. Nucl. Mater. 240 (1996) 75.
[9] V.Kh. Alimov et al., J. Nucl. Mater. 375 (2008) 192.
[10] M. Sakamoto et al., Nucl. Fusion 42 (2002) 165.
[11] H. Zushi et al., Nucl. Fusion 45 (2005) S142.
[12] R. Bhattacharyay et al., Nucl. Fusion 47 (2007) 864.
[13] T. Loarer, Nucl. Fusion 47 (2007) 1112.
[14] E. Titrone, J. Nucl. Mater. 363–365 (2007) 12.
[15] Y. Hirooka et al., J. Nucl. Mater. 363–365 (2007) 775.
[16] T. Shikama et al., Phys. Plasma 14 (2007) 072509.
[17] H. Iwakiri et al., J. Nucl. Mater. 307–311 (2002) 135.
[18] K. Tokunaga et al., J. Nucl. Mater. 337–339 (2005) 887.
[19] R.A. Causey et al., J. Nucl. Mater. 337–339 (2005) 600.